Wetland Mapping by Fusion of Deep learning and Ensemble Model for Enhancing Prediction Outcomes

Thylashri S.[1]*, Rajalakshmi N. R.[2]

[1,2] Department of Computer Science and Engineering, Vel Tech Rangarajan Dr Sagunthala R&D Institute of Science and Technology, Avadi, Chennai, Tamil Nadu, India
Emails:thyla.csrd@gmail.com; researchwork411@gmail.com

Abstract

Constraints perceived in different socioeconomic situations reinforce land use patterns and land cover (LULC) at different levels. However, the statistical information regarding the LULC variations encounters enormous significance for the execution and modelling of appropriate environmental variations and resource management with the available remote sensed data from diverse satellite images and advanced computing technologies; information is generally retrieved from the image classification approaches. However, a broader quantitative analysis of various classification approaches is crucial to choosing an effectual classifier model to acquire appropriate land use regions. We concentrate on the Karavetti region and its related fields in this study. We use a Non-Linear Recurrent Convolutional Neural Network (NLR-CNN) to analyze the data statistically. Well-known techniques such as Support Vector Machine (SVM), Random Forest (RF), and Decision Tree (DT), among others are used to evaluate the model performance. High-resolution images and the data points supplied are also used to assess the accuracy of the categorization and prediction. A confusion matrix is generated where the land cover regions show superior classification accuracy with the fusion model. Also, the NDVI facts and additional metrics like loss, error rate and kappa coefficients are analyzed. Therefore, the outcomes show that the anticipated is considered more robust with better performance to enhance the classification accuracy with the specific land cover regions.

Keywords: land cover; land use; classification; learning approaches; and fusion-based prediction

1. Introduction

Because of its ability to capture biotic and abiotic variables that closely resemble biological conditions on the ground, land use and land cover monitoring (LULC) is paramount [1]. In addition, LULC provides information about the earth's surface. A more accurate understanding of the relationships between human activities and the physical environment is made possible through the precise LULC mapping, which improves environmental change assessment. However, despite LULC products' accessibility and quantity, they have serious errors. For instance, it is reported that datasets like FROM-GLC, MCD12Q1, GLC2000, and GlobeLand30 have overall accuracy rates of 64.9%, 78.8%, 77.9%, and 80.3%, respectively [2]. As a result, it still needs to be completed to evaluate and integrate different land-use and land-cover (LULC) outputs, especially in the context of hydrological, climatological and ecological studies, including climate change research [3]. In research on precipitation, the accuracy of land-cover data is critical, with results being considerably affected when accuracy falls below 80% and further degrading as accuracy lowers. Unfortunately, most datasets are insufficiently accurate for general and class-specific regional climate modelling requirements. Studies have also shown that the accuracy of these data in Karavetti is significantly worse than in other areas [4], thus failing to meet the stringent criteria for optimal use of this region. This limitation hinders further development of studies on desertification monitoring, ecosystem services assessment, and regional climate simulations [5]. To address this problem, highly accurate land cover datasets must be created. It combines existing land use, land cover, and auxiliary datasets to produce realistic climate simulations [6]. To overcome these restrictions, this research aims to put forth a technique for ensemble learning in the classification of land use and land cover (LULC), an area with complex topography characteristics [7]. In addition to Landsat 8 OLI imagery, several geographic datasets are used to produce a set of highly accurate land cover data, including extended vegetation index (EVI), net primary productivity (NPP), leaf area index (LAI), FROM-GLC, MCD12Q1, ESA-LC, and a digital elevation model (DEM) [8]. Northwest province was selected and divided into three sub-regions due to its complicated topography and climate to demonstrate the applicability

Doi: https://doi.org/10.54216/FPA.140115
Received: June 16, 2023 Revised: October 16, 2023 Accepted: November 26, 2023

of the proposed strategy. Different ensemble learning strategies were then developed for each subregion [9]. The settings of the machine learning algorithms were determined, training samples were collected, and the classification accuracy of each land use and land cover (LULC) classification enabled by ensemble learning was evaluated [10]. Various classification methods, including K-nearest neighbour (KNN), decision trees (DTs), random forests (RF), support vector machines (SVM), artificial neural networks (ANN), and extreme learning machines, are widely used in remote sensing [11]. Various machine learning methods have significant advantages in identifying specific land use and land cover types (LULC) due to the complex nature of remote sensing data from multiple sources. A single classifier cannot significantly improve the accuracy of all LULC classes [12]. As a result, finding the best classification methods is still a challenge. For instance, it was discovered that the accuracy of SVM in categorizing irrigated plants in a given LULC classification within a specific area was 92%. In contrast, it was only 72% for oak woods [13] – [15].

The remote sensing image analysis branch is paying much attention to classifier ensembles, often known as multiple classifier systems. They may use the benefits of several classifiers while minimizing their drawbacks to achieve high classification accuracy. Various combinatorial methods have been developed, often used to combine different classes. For example, in a study, an ensemble learning classification model was built by combining C4.5, support vector machines (SVMs), decision trees (DTs), and artificial neural networks (ANNs). Compared to other simple classifiers, their model had a better overall accuracy (OA) of 88.12% and a kappa value of 0.88. In another study, the author showed how ensemble technology increased the stability and classification abilities of individual ANNs. To categorize land use and land cover (LULC) in the wetlands of Karavetti, they used two ensemble techniques based on ANNs. The main contributions of this study are the development of a novel ensemble learning method and the incorporation of topographic parameters in the categorization of land cover in Karavetti. In addition, we have developed a novel land cover product that solves the problem of low accuracy of land cover categorization in climate simulation of Karavetti by using a two-stage classification approach. Other industries, such as spatial planning and hydrological modelling, could also use this product. The study results will improve our knowledge of the atmosphere-land interaction in arid regions. The accuracy of LULC classification is closely related to the classification method chosen and the remote sensing data used. With the improvement of processing power and remote sensing technologies, machine learning has moved up the list of methods for LULC classification.

Additionally, the characteristics of the research area and the kind of associated material impact the performance of classification algorithms. Therefore, to maximize the effectiveness of multiclassifier ensemble learning, it is crucial to consider both the machine learning method and the properties of the feature data. Machine learning algorithms are ultimately more efficient and successful than traditional classification approaches since they are not based on standard assumptions or statistical traits. However, selecting the appropriate classification algorithm for a particular sector is still vital. To compute the effects of driving forces based on environmental changes, analyze the connection between the environment and humans, and assess both positive and negative variation, LULC regional mapping is required. Geographic Information Systems (GIS) and Remote sensing are recognized as powerful tools that aid in the collection of LULC data because they are accurate, cost-effective, real-time, and offer a high degree of geographical coverage. Because it is readily available and has a higher resolution, remote sensing data is frequently used in LULC research. However, the need for a classifier or classification system makes improving forecast accuracy using crucial indicators challenging. The significant research contributions are:

1) An analysis is done with the real-time data gathered from Karavetti using modern Machine Learning approaches;

2) Here, classification is done with the novel Non-Linear Recurrent Convolutional Neural Network (NLR-CNN), where SVM, DT and RF act as the baseline classifiers;

3) The anticipated model is evaluated and compared with other approaches, establishing a better trade-off.

The work is structured as follows: section 2 provides a broader analysis of various prevailing approaches. The methodology is demonstrated in section 3, with investigational outcomes in section 4. The summary is provided in section 5 with ideas for future research.

2. Related works

The geography research most thoroughly examined is the LU/LC change categorization. Different categorization methods are utilized to embed on the planet's surface. Since it helps characterize different LU/LC types using satellite imagery, the topic of LU/LC change categorization has been investigated for decades [16]. To categorize LU/LC variation, researchers used supervised, unsupervised, metric, quasi, object-oriented, per-pixel, template, and complex learners [17] – [18].

Doi: https://doi.org/10.54216/FPA.140115
Received: June 16, 2023 Revised: October 16, 2023 Accepted: November 26, 2023

Land usage and land cover are distinguished on indigenous land maps. Each is distinguished from the others by the thorough description. According to the Food and Agriculture Organisation of the United Nations (FAO) [19], Land use refers to the human activities, structures, and resources used to create, modify, or maintain a particular land cover category. Land cover refers to the physical cover of the earth's surface [20]. The definition states that land use and cover are closely related, so their classification is unavoidable. However, these two concepts are frequently used in error by one another [21]. As a result, current research has seen the "land use and land cover" (LULC) categorization as a more detailed term incorporating this connection. Depending on the best purposes, different categorizations exist for LULC; one of the most well-known interpretations comes from the FAO and offers an LCLU which allows for different knowledge levels to be compensated by starting with organized general categories and then further methodically developing land into more comprehensive sub-classes [22]. This specification also assures a high level of mappability by integrating consumer land use features. Most studies that categorize land cover or land use focus on several plant cover or land use subcategories [23]. These classifications are at a higher level of organization depending on the intended use, differentiating apparent land coverings or concentrating on specific land cover subtopics. Examples of software LULC classification approaches available in the literature include wetland classification, urban land-use classification, farm categorization, forest categorization, and other vegetation maps. In [24], mapping the land uses to the ground surface using aerial film was the first instance where satellite data was used for the LULC classification.

Years later, soon after the launch of the Landsat programme and the deployment of the Environmental Protection Technologies research plane with a multispectral scanner (MSS), investigations using remote-sensing imaging data to classify the LULC advanced to a new level. In actuality, the Landsat project and (private) data dissemination introduced new issues of inter-different datasets, land mapping and monitoring on a temporal basis, and ecology uses of satellite data to the area of LULC [25]. The author describes some of the early attempts on these issues. Studies on LULC identification and its extra challenges are continuously and rapidly changing (AI) due to significant improvements in computer power and memory capacity and the advent of AI [26]. Furthermore, data quality and remote sensing technology advances allow researchers to extract information from large amounts of data [27]. Hyperspectral images were later adopted by the Earth Observation community as processing capabilities and digitization advances reduced their complexity and time requirements. However, an increasing number of professionals are becoming interested in LULC identification due to the immense potential of such data and the quick improvements in computing technology [28].

The incredible successes of deep learning since the Net Large Scale Visual Recognition Challenge (ILSVRC) have inspired satellite scientists to utilize comparable methods on remotely sensed data [29]. The author explores the present state of deep learning techniques for hyperspectral categorization while concentrating on the challenges of multispectral imaging technology. Additionally, the author describes machine learning architectures for categorizing s and evaluates them using widely-used samples. This review examines the new research utilizing deep learning algorithms for panchromatic and spectroscopic image classification [30]. The primary objective is to produce a study that is interesting to read and explains how to evaluate the present state of deep learning in the LULC classification of remote sensing data, emphasizing spectroscopic and panchromatic images. This paper aims to provide readers with a place to find the approaches and datasets needed to address the field's challenges.

3. Methodology

The proposed NLR-CNN is explained in detail in the following section. The shallow subnetwork for feature extraction and the deep subnetwork for feature fusion are separate subnetworks that form this end-to-end network.

3.1. Feature representation

A shallow feature extraction subnetwork that can extract spatial features from multisequence data band by band is part of the proposed NLR-CNN. This method treats the multispectral images as a single set of multisequence data. Consequently, images with different band configurations (four or eight bands) can be trained without changing the structural parameters of the network. A tensor of size $B \times H \times W \times (M + 1)$ is used to describe the multisequence data, where B is the batch size, H is the height of the data, W is its width, and $M + 1$ is the total number of data samples. The characters xi identify Each data sample ($i = 1, 2, \ldots, M + 1$). The multisequence data are collected using the following techniques. As shown in Eq.(1), the original image ($H/S \times W/S \times M$) is first scaled down to the size of the image ($H \times W \times 1$) at scale S. The data is then processed into a multisequence image. The input data, denoted as multisequence data x_i, is then created by combining the upscaled ($H \times W \times M$) and ($H \times W \times 1$) as explained in Eq. (2).

Doi: https://doi.org/10.54216/FPA.140115
Received: June 16, 2023 Revised: October 16, 2023 Accepted: November 26, 2023

$$\left(\frac{H}{S} * \frac{W}{S} * M\right) \rightarrow \ (H * W * M) \tag{1}$$

$$x_i = \{\tilde{\imath}, \quad i\} \text{ where } i = 1,2, \dots, M+1 \tag{2}$$

A subnetwork with a convolutional neural network (CNN) as the basic structure is chosen to extract flat features. The image contains more spectral information. However, spatial-spectral features can be seen in the provided images. To extract spatial features from the given images, this sub-grid is used. Creating the sub-grid with the same parameters and structure significantly reduces the non-adaptive situation, and the grid parameters are minimized. Moreover, since the flat subnetwork is used for feature extraction band by band, the convolutional layers are processed sequentially. The usefulness of residual learning in feature extraction from images has been proven. Therefore, the shallow subnetwork for feature extraction contains the residual block. The residual block in Fig 1 consists of a skip connection and two convolutional layers. A ReLU activation function follows each convolutional layer. The operating principle of the residual block can be described as follows:

$$y_i = h(x_i) + R(x_i, B_i) \tag{3}$$

$$x_{i+1} = F(y_i) \tag{4}$$

In this study, the input and output of each residual block, represented as x_i and x_{i+1}, respectively, are processed by the residual function $R(.)$ in conjunction with the activation function $F(y_i)$ and the identity mapping function $h(x_i)$. The parameters of the residual block are shared to maximize accuracy and reduce the number of operations (NOPs). The feature map f_i (where i ranges from 1 to $M + 1$) is generated by the shallow feature extraction network φ, which extracts features from the multisequence data x_i.

$$f_i = \emptyset(x_i) = i = 1,2, \dots, M+1 \tag{5}$$

All convolutional layers in this network use $3 * 3$ convolution kernels, and no normalization layers are present. The activation function used in this network is the parametric ReLU [31].

3.2. Feature fusion

The feature maps for all bands are acquired after the initial extraction of shallow features, coupled with the spatial images and the spectral data from multispectral (MS) images. These feature maps are directly combined in several deep learning-based techniques to capture spectral and spatial properties. Given the high correlation and complementary information that these feature maps give, it is crucial to understand the interactions between them. Several recurrent neural networks (RNN), such as Long Short Memory (LSTM), Gated Recurrent Unit (GRU), ConvGRU and NLR-CNN, have been developed to efficiently capture the correlation between the spectral and spatial features of different bands. NLR-CNN stands out among these methods because it is particularly suitable for processing two-dimensional multisequence data. This study processes the two-dimensional multisequence data of all bands considered feature maps using a deep feature fusion subnetwork built on the NLR-CNN model. The NLR-CNN model allows interactions within and between different views, which facilitates the detection of local and global correlations across many bands. The proposed deep feature fusion subnetwork also keeps the spatial resolution of the input and output constant. Fig 1 shows a schematic design of the NLR-CNN model. Each feature map, represented by the letters f_i (where $i = 1, 2, \dots, M + 1$), has an update gate (Z_i) and a reset gate (RI) attached to it. A logic gate called the update gate (z_i) chooses the update activation (h_i).

$$z_i = \sigma\left(W_z * f_i + U_z * h_{i-1}\right) \tag{6}$$

In this case, the activation function (σ) is employed. The update gate incorporates the weight matrices (W_z) and (U_z), respectively. W_z represents the current input layer's connection to the hidden layer, while U_z represents the previous hidden layer's connections to the existing hidden layer. h_{i-1} represents the output activation from the previously hidden layer, symbolically representing the convolution operation. The candidate activation ($\tilde{h}_i$) is either taken into account or disregarded when calculating the prior activation $\tilde{h}_i$ with the reset gate (r), denoted as $(*)$.

$$r_i = \sigma\left(W_r * f_i + U_r * h_{i-1}\right) \tag{7}$$

Doi: https://doi.org/10.54216/FPA.140115
Received: June 16, 2023 Revised: October 16, 2023 Accepted: November 26, 2023

The weight matrix W_r represents the input layer, and the hidden layer is represented by U_r, which corresponds to the links between the input layer and the current hidden layer. The candidate activation, $\tilde{h}_i$, is expressed by the function $[f_i, h_{i-1}]$.

$$\tilde{h}_i = \tanh(W_h * f_i + U_h * (r_i - h_i - 1)) \quad (8)$$

In this study, the weights for the input, hidden, and previously hidden layers to the present hidden layer are called W_h and U_h, respectively. The hidden state of the cell's output activation h_i is determined by attempting to receive a specific expression $[h_{i-1}, \tilde{h}_i]$ using the Hadamard operator. The NLR-CNN model's convolution kernel is of size 3.

$$h_i = (1 - z_i) * h_{i-1} + z_i + \tilde{h}_i \quad (9)$$

The deep feature fusion subnetworks use the formulas outlined in Eq. (7) to Eq. (9) to process all band feature maps denoted by f, resulting in the output feature fusion represented by $\tilde{f}$. The resulting resolution is partially adjusted to the desired level by global average pooling [32] and referred to as A. A convolutional layer with $1 * 1$ convoluted kernel produces the sharpening result.

$$f = \tilde{f}/M + 1 \quad (10)$$

The feature fusion findings are subsequently transformed into a high-resolution image using this convolutional layer, which functions as a decoder.

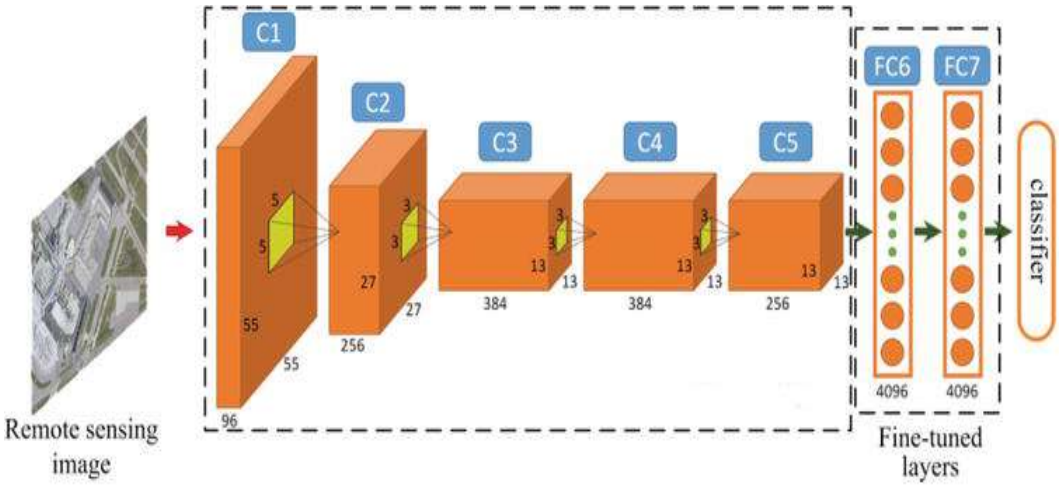

Figure 1: Proposed architecture

3.3. Ensemble Machine learning approaches

This section provides an overview of the theoretical basis for the ensemble learning techniques used for classification in the current research. Please refer to the cited sources if you want to learn more about the theoretical basis of an algorithm. An example of an ensemble learning technique is the SVM developed by Vapnik (1990s). SVM was first used to detect pattern recognition tasks, particularly the detection of handwritten numerals. SVM has several advantages: low training sample requirements, noise tolerance, adaptability to high-dimensional data and high stability. It is also well-known for producing accurate results when modelling complex non-linear decision boundaries. SVM is a supervised learning technique in various remote sensing applications. Random Forest (RF) is a classification method combining different classifications and regression trees through a bagging process. This method eliminates generalization errors and enhances classification accuracy, making it an effective multi-sourced remote sensing classification (MRS) method. Due to its high level of precision, RF has been widely used in LULC classification. Please refer to the relevant literature for a comprehensive explanation of RF. The Iterative Dichotomiser 3 technique has been updated to create the decision tree algorithm C4.5. It is intended to

Doi: https://doi.org/10.54216/FPA.140115
Received: June 16, 2023 Revised: October 16, 2023 Accepted: November 26, 2023

classify data from many remote sensing picture sources precisely. A robust logical framework, simple rules, and effective noise suppression are all hallmarks of C4.5. Please refer to the supplied for more information on C4.5. The concept of ensemble learning uses the additive influence of advantageous qualities to improve classification and predict performance. This strategy involves simultaneously training many machine learning algorithms. Ensemble learning does this by addressing the issue of overfitting that could develop when depending on a single classifier in situations with little data. This method also makes the most of the benefits that each classifier has to offer.

3.4. Dataset

The LULC classification at the regional level is often based on the wide availability and comprehensive coverage of Landsat satellite-image data. As most phenological changes are observed, the use of the images from the Geological Survey was selected for this investigation. The time frame chosen for LULC categorization was from April to August. The ESG (Enhanced Vegetable Index), NDBI (Normalized Difference Building Index), and MNDWI (Enhanced Normalised Water Index) were generated from Landsat bands, respectively. The composite spectral index from Landsat 8 was also used. In addition, the current study included information from four more LULC information sources.

3.5. Spatial analysis

Consistency analysis and geographical attribute extraction were the primary approaches in this study. A distinct spatial data mining inference rule was developed to distinguish between land use and land cover groups (LULCs), relying on grid consistency. To aid in the zoning shape of LULC categorizations, (0.25 km^2) was initially generated using the ArcGIS version 10.2; four LULC products were then extracted, as well as a plant type and additional data by extracting multiple value points from feature points. The resulting net data consisted of 13 distinct attribute information types, which were then aggregated with net feature points, net data, and spatial consistency levels for vegetation type maps using a grid comparison approach for categorization systems.

4. Numerical results and analysis

The primary criterion for assessing the performance of machine learning algorithms is classification performance. A confusion matrix was employed to calculate multiple evaluation metrics, including OA, PPA, UA, and Kappa, to determine the classification capability of various algorithms and ensembled learning approaches. The formulae used to estimate these metrics were as follows:

Field surveys and visual examinations are considered the most effective sample selection techniques to achieve high accuracy for land-cover classification. To meet the requirements of this study, sampling points were selected from across Karavetti.

$$OA = \frac{1}{N}\sum_{i=1}^{r} X_{ii} \tag{11}$$

$$UA_i = \frac{X_{ii}}{X_{+i}} \tag{12}$$

$$PA_i = \frac{X_{ii}}{X_{i+}} \tag{13}$$

$$Kappa = \frac{N\sum_{i=1}^{r} X_{ii} - \sum_{i=1}^{r}(X_{i+} * X_{+i})}{N^2 - \sum_{i=1}^{r}(X_{i+} + X_{+i})} \tag{14}$$

Here, N represents the number of training samples; r is the row count of the confusion matrix; X_{ii} is the number of samples of rows i and i, i is the diagonal intersection, and X_{+i} and X_{i+} are the marginal totals of the rows r and i respectively. OA and Kappa are the most commonly used metrics to assess classification accuracy. However, they may not provide independent samples for calculation purposes. Therefore, it is necessary to use the same test set to evaluate the accuracy of each map under each circumstance. Paired Z-score testing was conducted to determine if the differences in classification accuracy between different ensemble learning methods were statistically significant at the 5% level. A Z-score above 1.96 was considered statistically significant. Google Earth and on-site field photography were used to identify the precise land cover type at each sampling location.

4.1. Parameter learning

Doi: https://doi.org/10.54216/FPA.140115
Received: June 16, 2023 Revised: October 16, 2023 Accepted: November 26, 2023

The cost (C) and weight (γ) parameters influence the RBF kernel of the SVM. On training and validation samples, the ideal combination of C (2−2, 2−1, 20, 21, 22, 23, 24, 25, 26, 27) and γ (2−5, 2−4, 2−3, 2−2, 2−1, 20, 21, 22, 23, 24) was investigated. The number of Ntree and Mtry are essential for RF classification. The Mtry value should be set to the inverse of the input variable and the Ntree value to the multiple of 500 to maximise the classification impact. Therefore, this study evaluated a range of Mtry values between 1 and 16 and Ntree values between 500 and 5000 (with 500 intervals). The number of Hidden Layer Nodes, adjusted from 1 to 50 in this experiment, significantly affects the accuracy of various machine learning algorithms for determining PA and UA of different LULC species. The Sigmoid activation function is employed to modify the neurons receiving input information to achieve non-linear prediction. As an alternative, C4.5's simplicity does away with the requirement for parameter sets.

4.2. Discussion

The objective of the present study was to create a set of ensemble learning models for LULC classification in the region of Karavetti and its sub-regions. The classification methods employed in this study were SVM, RF, and C4.5. The comparison of the OA and Kappa values was used to evaluate the efficacy of each ensemble technique. Table 1 lists the findings for OA and Kappa. Notably, this region showed the most significant improvement in the LULC classification accuracy, with OA and Kappa values rising by roughly ≥ 7% and 8.5%, respectively. The sub-regions with the next-highest improvements had OAs that increased by ≥ 6 and 5.5% and Kappas that increased by ≥ 6.7 and 6%, respectively. In the southern region, there was the most significant improvement in overall accuracy, with increased OA values by more than five percentage points and Kappa values by six percentage points. As a result, it was determined that ensemble learning classification using a variety of single classifier combinations could significantly enhance LULC classification accuracies in three sub-regions and wetland regions. Furthermore, the ensemble strategy employing algorithms like SVM, RF and C4.5 resulted in significantly higher overall accuracy and Kappa values than any other ensemble approach using only three methods. In particular, all three regions saw an increase in OA values ranging from 2-2.5 percentage points, 2-3 percentage points, and in Kappa values ranging from 3-5 percentage points, 3-6 percentage points. In contrast, the Northern region's OA values increased by less than 1.00 percentage points, up to 0.80 percentage points, and the Kappa values increased by less than 0.48 percentage points. It is crucial to remember that choosing the correct number and kind of classifiers is essential for achieving the most significant classification performance.

The prevalence and number of classifiers play a significant role in ensemble learning. According to the significance tests, there is a strong correlation between the Z scores of the various ensemble learning combinations used across the Karavetti region and its subregions. The study revealed significant differences between northern and southern areas based on whether three learning algorithms were used. The differences between the regions were statistically significant when the Z scores exceeded or exceeded 1.96, and the p −values were below or greater than 5%. However, there was no significant difference between the north and south parts. The ensemble learning strategy was the most effective for the sub-regions. In particular, the overall accuracy of Southern and Northern was significantly higher than the Karavetti region when compared to ensemble learning classification with an increase of 7%, respectively. Consequently, when the geographical division of Karavetti was made based on topographical conditions, the misinterpretation of plant types due to variations in topographical features or highly varying surface vegetation was significantly reduced in LULC classification across the heterogeneous states of Karaivetti.

Table 1: OA and Kappa coefficient

Methods	Entire region		Northern region		Central Region		Southern region	
	OA	Kappa	OA	Kappa	OA	Kappa	OA	Kappa
k-NN	88	85	94	94	79	75	93	91
SVM	86	83	91	90	91	90	91	90
RF	86	84	92	92	91	88	93	91
ANN	85	82	93	88	90	87	93	89
C4.5	87	83	90	92	91	88	91	91

Doi: https://doi.org/10.54216/FPA.140115
Received: June 16, 2023 Revised: October 16, 2023 Accepted: November 26, 2023

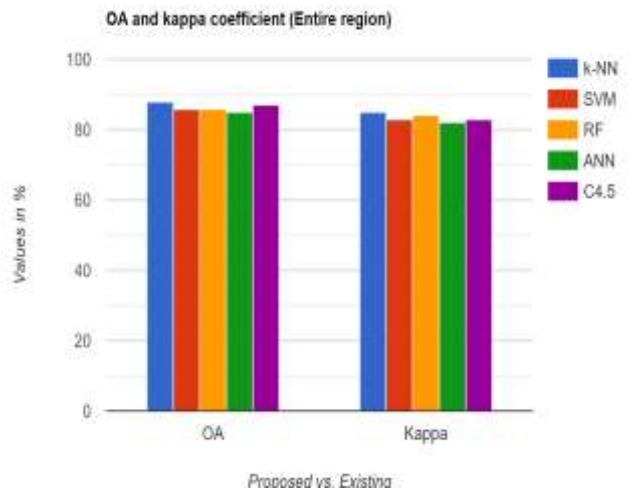

Figure 2a OA and Kappa coefficient of Entire Karavetti region

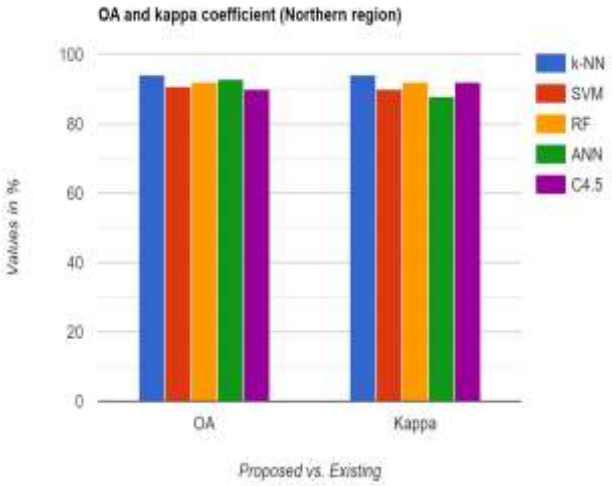

Figure 2b OA and Kappa coefficient of Northern Karavetti region

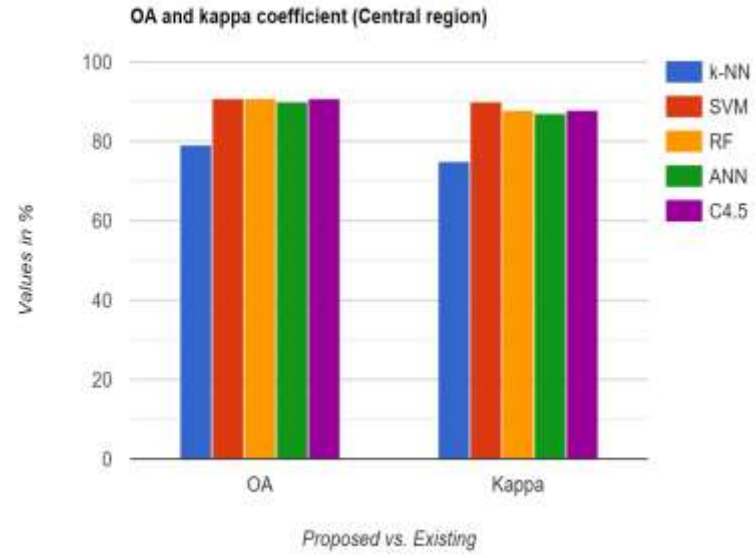

Figure 2a OA and Kappa coefficient of Central Karavetti region

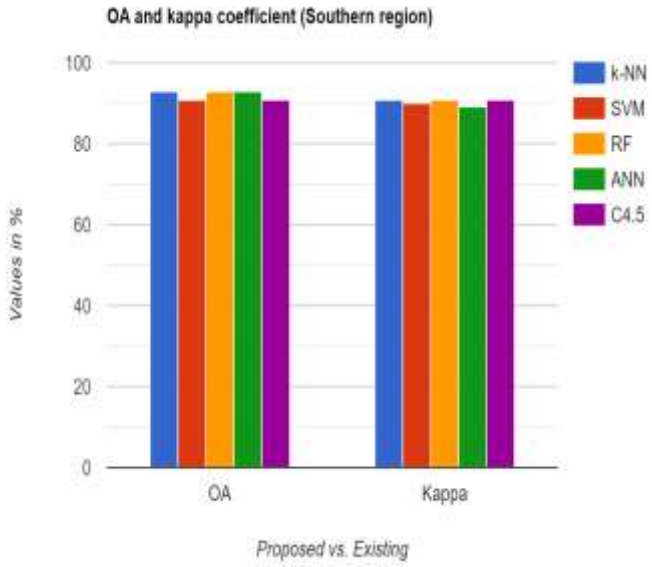

Figure 2a OA and Kappa coefficient of Southern Karavetti region

Table 2 OA and Kappa coefficient for Ensemble analysis

Methods	Entire region		Northern region		Central Region		Southern region	
	OA	Kappa	OA	Kappa	OA	Kappa	OA	Kappa
SVM, RF, ANN	91	88	96	96	94	94	96	96
SVM, RF, C4.5, ANN	88	86	95	95	94	93	96	97
SVM, C4.5, ANN	90	89	95	95	94	93	96	96
RF, C4.5, ANN	91	89	95	95	94	92	96	96
SVM, RF, C4.5,	93	91	96	95	96	96	97	96

Doi: https://doi.org/10.54216/FPA.140115
Received: June 16, 2023 Revised: October 16, 2023 Accepted: November 26, 2023

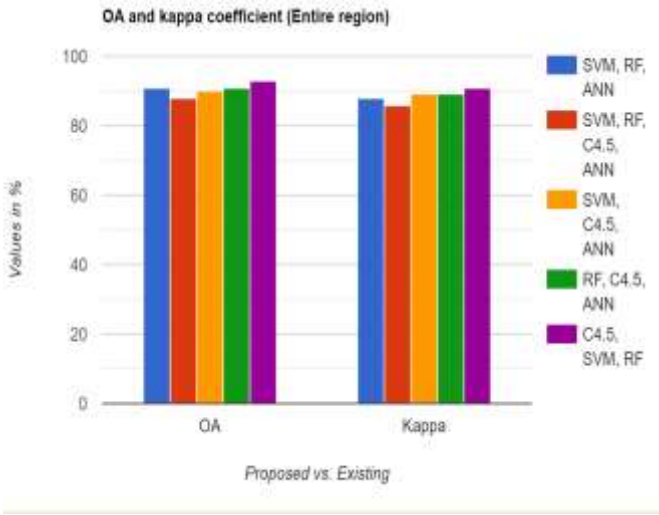

Figure 3a OA and Kappa coefficient of Entire Karavetti region with Ensemble learning

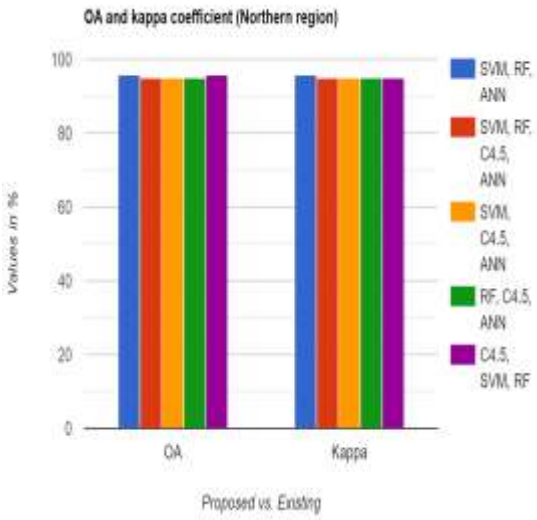

Figure 3b OA and Kappa coefficient of Northern Karavetti region with Ensemble learning

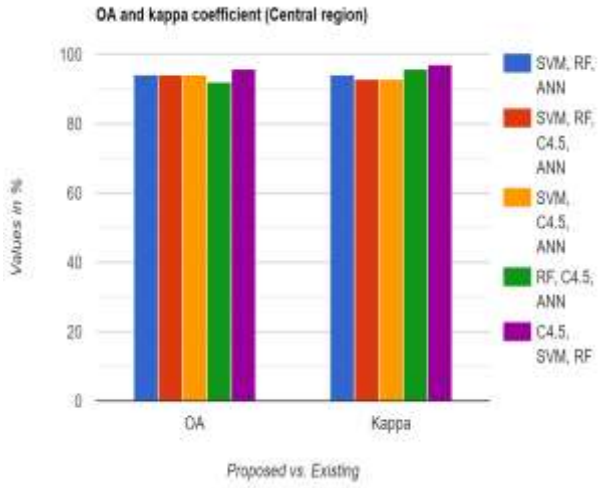

Figure 3c OA and Kappa coefficient of Central Karavetti region with Ensemble learning

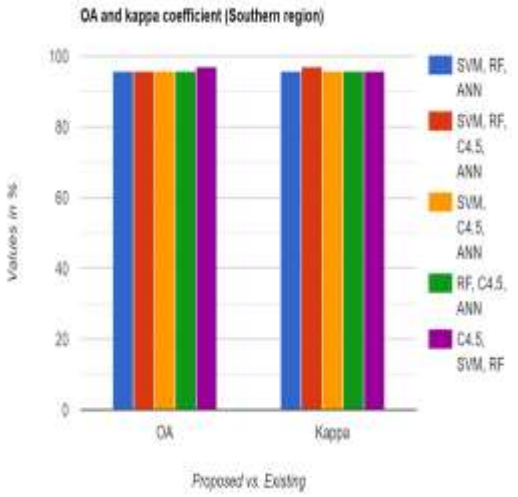

Figure 3d OA and Kappa coefficient of Southern Karavetti region with Ensemble learning

4.3. Ensemble effects on classification

In the region of Karavetti, ensemble learning techniques were employed to significantly improve the accuracy of land use and LULC categories compared with ML classification. Fig 2 to Fig 3 illustrates the improvements in the accuracy of various land classes. Wetlands in these regions experienced significant improvements in their accuracy, ranging from 4% to 25%, while urban, industrial and mining environments experienced improvements from 5% to 15%. Like urban regions, industrial and mining areas witnessed improvements of 15% and 12%, while others showed gains of 13% and 20%, respectively. Urban areas also saw 12% and 13% increases in PA and UA. The impact of Northern regions on the growth of primary productivity (PA) and urban areas (UA) to various sub-regions was comparable to that of the Karavetti region for different land cover types. Notably, the improvement for plantation varied from 9% to 20% for PA and from 9% to 14% for UA. Similar improvements were made in urban regions, 16% and 12%, respectively. The improvements were 22% and 19% for paddy fields, 18% and 19% for industrial and mining sectors, and 12% and 14% for cold. This region experienced the most significant growth in PA and UA among the sub-regions, with gains ranging from 6% to 24% for PA and 6.5% to 18% for UA. The ensemble learning approach outperformed individual classifiers in the classification accuracy of Paddy Fields (18%), Mining and Industrial (21%), Permanent Wetlands (15%), and Paddy Fields (16%), Industrial and Mining (14%), and Permanent Wetlands (18%), and cold (21%), with the most significant improvements in Southern (PA and UA, 6% and 6%).

Doi: https://doi.org/10.54216/FPA.140115
Received: June 16, 2023 Revised: October 16, 2023 Accepted: November 26, 2023

Table 2 compares the POA and Kappa of Karavetti and its sub-region. Compared to the entire region, sub-region ensemble learning produced noticeable trends in improving land types. At first, paddy fields, dry land, permanent wetlands, and shrublands all showed considerable gains, with average increases in PA and UA of 7.5%, 7.2%, 11%, and 7%, respectively. The difficulty of correctly identifying the same vegetation types in Karavetti was overcome by ensemble learning at the sub-regional level. This method decreased surface spectral variation within a given vegetation type, thus enhancing classification accuracy. This outcome may have been affected by differences in spectral characteristics among different geographical locations. Furthermore, the study revealed that, within a single or two specific zones, evergreen, deciduous, broadleaf forest, grassland, cropland, natural vegetation mosaic, rural environment, urban environment, industrial and mining environment all had positive contributions. In contrast to the other two sub-regions, however, the classification of grasslands significantly improved in the northern region. However, none of the sub-regions showed much improvement in cold and water conditions; some even exhibited negative correlations. It may result from these land cover kinds' distinctive traits, which can be determined without ensemble learning approaches. The minor drop in accuracy can result from spectral signatures being over-fitted for particular terrain classifications. A lack of training data may have also constrained the effectiveness of ensemble learning under these complex topographic settings.

5. Conclusion

This study developed a group learning approach for LULC classification in the northwest region of Karavetti, Ariyalur. Combining three machine learning algorithms, the goal was to investigate various ensemble learning strategies. Three distinct sub-regions were identified based on the research area's geographical and climatic characteristics. The study and analysis of the ensemble learning strategies yielded three main conclusions. Firstly, the suggested ensemble-based learning strategy significantly increased LULC classification accuracy compared to single machine learning methods. The most significant effect was seen in the subregion of Karavetti, where the OA and Kappa values increased from 6% to 7%. Subsequently, Southern Karavetti was the next sub-region to experience an increase in OA and Kappa, with values growing from 5 to 5.5%. The ensemble learning approach with NLR-CNN was employed to achieve higher classification accuracy, necessitating the correct classification of various forest types. Furthermore, the study focused on improving LULC classification in different sub-regions. The most potent learning approaches were used to identify the most accurate ensembles for each sub-region, ranging from 96.5% to 97%. SVM, RF, and C4.5 were the most commonly used algorithms. This study highlights the importance of considering the complex topographical characteristics of Karavetti when determining the accuracy of land cover classification. The ensemble learning technique, which yielded the highest accuracy of 96.5%, was specifically selected for its use of SVM, RF and C4.5. A new product was also developed based on a two-tiered classification method and a new ensemble learning approach. This work addresses the low accuracy of land-cover classifications for climate simulations in Karavetti and offers potential applications in areas such as wetland mapping, spatial planning and hydrologic modelling.

References

[1] Mohammadimanesh, B. Salehi, M. Mahdianpari, B. Brisco and M. Motagh, "Multi-temporal multi-frequency and multi-polarization coherence and SAR backscatter analysis of wetlands," ISPRS J. Photogramm. Remote Sens., vol. 142, pp. 78-93, 2018.

[2] Mahdianpari et al., "Fisher linear discriminant analysis of coherency matrix for wetland classification using PolSAR," Remote Sens. Environ., vol. 206, pp. 300-317, 2018.

[3] M. Belgiu and L. Drăguţ, "Random forest in remote sensing: A review of applications and future directions," ISPRS J. Photogramm. Remote Sens., vol. 114, pp. 24-31, 2016.

[4] Mahdianpari, B. Salehi, F. Mohammadimanesh and B. Brisco, "An assessment of simulated compact polarimetric SAR data for wetland classification using random forest algorithm," Can. J. Remote Sens., vol. 43, no. 5, pp. 468-484, 2017.

[5] Y. Jia et al., "Caffe: Convolutional architecture for fast feature embedding," Proc. 22nd ACM Int. Conf. Multimedia, pp. 675-678, 2014.

[6] Amani, M., B. Salehi, S. Mahdavi, and B. Brisco. 2018. “Spectral Analysis of Wetlands Using Multi-Source Optical Satellite Imagery.” ISPRS Journal of Photogrammetry and Remote Sensing 144: 119–136.

[7] Davis, P., F. Aziz, M. T. Newaz, W. Sher, and L. Simon. 2021. “The Classification of Construction Waste Material Using a Deep Convolutional Neural Network.” Automation in Construction 122 (February): 103481.

Doi: https://doi.org/10.54216/FPA.140115
Received: June 16, 2023 Revised: October 16, 2023 Accepted: November 26, 2023

[8] Berhane, T. M., C. R. Lane, Q. Wu, B. C. Autrey, O. A. Anenkhonov, V. V. Chepinoga, and H. Liu. 2018. "Decision-Tree, Rule-Based, and Random Forest Classification of High-Resolution Multispectral Imagery for Wetland Mapping and Inventory." Remote Sensing 10 (4): 580.

[9] Jamali, A. 2020a. "Land Use Land Cover Mapping Using Advanced Machine Learning Classifiers: A Case Study of Shiraz City, Iran." Earth Science Informatics 13 (4): 1015–1030.

[10] Ji, S., C. Zhang, A. Xu, Y. Shi, and Y. Duan. 2018. "3D Convolutional Neural Networks for Crop Classification with Multi-Temporal Remote Sensing Images." Remote Sensing 10 (2): 75.

[11] Liu, K., S. Wu, Z. Luo, Z. Gongze, X. Ma, Z. Cao, and H. Li. 2021 February. "An Intelligent Fault Diagnosis Method for Transformer Based on IPSO-GcForest." In Mathematical Problems in Engineering 2021, edited by M. Kunicki. Hindawi: 6610338.

[12] Mahdianpari, M., B. Salehi, F. Mohammadimanesh, and M. Motagh. 2017. "Random Forest Wetland Classification Using ALOS-2 L-Band, RADARSAT-2 C-Band, and TerraSAR-X Imagery." ISPRS Journal of Photogrammetry and Remote Sensing 130: 13–31.

[13] Mahdianpari, M., B. Salehi, M. Rezaee, F. Mohammadimanesh, and Y. Zhang. 2018. "Very Deep Convolutional Neural Networks for Complex Land Cover Mapping Using Multispectral Remote Sensing Imagery." Remote Sensing 10 (7): 1119.

[14] Sherubha, "Graph-Based Event Measurement for Analyzing Distributed Anomalies in Sensor Networks," Sådhanå(Springer), 45:212, https://doi.org/10.1007/s12046-020-01451-w

[15] Sherubha, "An Efficient Network Threat Detection and Classification Method using ANP-MVPS Algorithm in Wireless Sensor Networks," International Journal of Innovative Technology and Exploring Engineering (IJITEE), ISSN: 2278-3075, Volume-8 Issue-11, September 2019

[16] Sherubha, "An Efficient Intrusion Detection and Authentication Mechanism for Detecting Clone Attack in Wireless Sensor Networks," Journal of Advanced Research in Dynamical and Control Systems (JARDCS), Volume 11, issue 5, Pg No. 55-68

[17] Maxwell, A. E., T. A. Warner, and F. Fang. 2018. "Implementation of Machine-Learning Classification in Remote Sensing: An Applied Review." International Journal of Remote Sensing 39 (9): 2784–2817.

[18] Rubec, C. 2018. "The Canadian Wetland Classification System." In Finlayson C.M. et al. (eds). The Wetland Book, 1577–1581. Dordrecht, The Netherlands: Springer.

[19] Song, H., X.-Y. Han, C. E. Montenegro-Marin, and S. Krishnamoorthy. 2021. "Secure Prediction and Assessment of Sports Injuries Using Deep Learning Based Convolutional Neural Network." Journal of Ambient Intelligence and Humanized Computing 12 (3): 3399–3410.

[20] Sun, X., P. Wang, C. Wang, Y. Liu, and K. Fu. 2021. "PBNet: Part-Based Convolutional Neural Network for Complex Composite Object Detection in Remote Sensing Imagery." ISPRS Journal of Photogrammetry and Remote Sensing 173 (March): 50–65.

[21] Wenping, M., Y. Hui, Y. Wu, X. Yunta, H. Tao, J. Licheng, and H. Biao. 2019. "Change Detection Based on Multi-Grained Cascade Forest and Multi-Scale Fusion for SAR Images." Remote Sensing 11 (2): 142.

[22] Zhang, J., and H. Song. 2021. "Multi-Feature Fusion for Weak Target Detection on Sea-Surface Based on FAR Controllable Deep Forest Model." Remote Sensing 13 (4): 812.

[23] Zhiyuan, S., M. Li, J. Zhang, B. Hu, G. Qi, and Y. Zhu. 2021. "Transient Voltage Stability Assessment Method Based on GcForest." Journal of Physics. Conference Series 1914 (1): IOP Publishing: 012025.

[24] Alqahtani, F., Abotaleb, M., Subhi, A.A. et al. A hybrid deep learning model for rainfall in the wetlands of southern Iraq. Model. Earth Syst. Environ. (2023).

[25] Zhang F, Fleyeh H, Bales C (2022) A hybrid model based on bidirectional long short-term memory neural network and Catboost for short-term electricity spot price forecasting. J Oper Res Soc 73(2):301–325

[26] Wang Y, Liao W, Chang Y (2018) Gated recurrent unit network-based short-term photovoltaic forecasting. Energies 11(8):2163

Doi: https://doi.org/10.54216/FPA.140115
Received: June 16, 2023 Revised: October 16, 2023 Accepted: November 26, 2023

[27] Song X, Liu Y, Xue L, Wang J, Zhang J, Wang J, et al. (2020) Time-series well performance prediction based on long short-term memory (LSTM) neural network model. J Petrol Sci Eng 186

[28] Seidu J, Ewusi A, Kuma J, Ziggah Y, Voigt H (2022) A hybrid groundwater level prediction model using signal decomposition and optimized extreme learning machine. Model Earth Syst Environ 8(3):3607–3624

[29] Reddy D, Prasad P (2018) Prediction of vegetation dynamics using NDVI time series data and LSTM. Model Earth Syst Environ 4(1):409–419

[30] Nie Q, Wan D, Wang R (2021) CNN-BiLSTM water level prediction method with an attention mechanism. J Phys 2078(1):012032

[31] Niclas Ståhl a b, Lisa Weimann, "Identifying wetland areas in historical maps using deep convolutional neural networks", Ecological Informatics, Volume 68, May 2022, 101557

[32]Kumar Mainali a, Michael Evans, David Saavedra, Emily Mills, Becca Madsen, Susan Minnemeyer, "Convolutional neural network for high-resolution wetland mapping with open data: Variable selection and the challenges of a generalizable model", Science of The Total Environment, Vol. 861, 25 February 2023, 160622

Doi: https://doi.org/10.54216/FPA.140115
Received: June 16, 2023 Revised: October 16, 2023 Accepted: November 26, 2023